Tomasz RYMARCZYK[1,2], Paweł NITA[2], Andres VEJAR[2], Barbara STEFANIAK[2], Jan Sikora[2]

University of Economics and Innovation (1),
Research & Development Centre Netrix S.A. (2),

Electrical tomography system for Innovative Imaging and Signal Analysis

Abstract. In this article, we describe the electrical tomography system for biomedical applications. Electrical tomography for pulmonology and heart monitoring is a non-invasive imaging method in which an unknown physical object is examined using electrical currents applied at the boundary. The internal conductivity distribution is recovered from the measured boundary voltage data. The numerical model of the lungs with heart is presented. The deterministic algorithms based on the SVD distribution and gradient techniques were analysed. The algorithms of electrical reconstruction of impedance tomography were tested. New results of the reconstruction of the numerically simulated phantom were presented. The calculations were made for the defined model by solving the inverse problem. The finite element method was used to solve the simple problem. The collection of tomographic data must be as fast as reliable to consider the possibility of real-time reconstruction. System architecture and prototype design for biomedical electrical tomography were also presented. The hardware solution was based on the FPGA chip. The system is a mobile solution that allows simultaneous recording of the electrical potential of cardiac function and lung ventilation.

*Streszczenie. W tym artykule opisujemy system tomografii elektrycznej do zastosowań biomedycznych. Tomografia elektryczna do monitorowania pulmonologii i serca jest nieinwazyjną metodą obrazowania, w której nieznany obiekt fizyczny jest badany za pomocą prądów elektrycznych stosowanych na granicy. Wewnętrzny rozkład przewodnictwa jest odzyskiwany ze zmierzonych danych napięcia granicznego. Przedstawiony został model numeryczny płuc o serca. Przeanalizowane zostały algorytmy deterministyczne oparte o rozkład SVD i techniki gradientowe. Zbadano algorytmy rekonstrukcji elektrycznej tomografii impedancyjnej. Przedstawiono nowe wyniki rekonstrukcji symulowanego numerycznie fantomu. Obliczenia wykonano dla zdefiniowanego modelu poprzez rozwiązanie zagadnienia odwrotnego. Do rozwiązania zagadnienia prostego zastosowano metodę elementów skończonych. Zbieranie danych tomograficznych musi być tak szybkie, jak niezawodne, aby uwzględnić możliwość rekonstrukcji w czasie rzeczywistym. Przedstawiona została również architektura systemu i projekt prototypów dla biomedycznej tomografii elektrycznej. Rozwiązanie hardware'owe oparto na układzie FPGA. System jest rozwiązaniem mobilnym, które umożliwia równoczesne rejestrowanie potencjału elektrycznego czynności serca i wentylację płuc. (**System tomografii elektrycznej do innowacyjnego obrazowania i analizy sygnału**).*

Keywords: Electrical Tomography, Inverse Problem, Image Analysis
Słowa kluczowe: tomografia elektryczna, zagadnienie odwrotne, analiza obrazów

Introduction

This article presents system architecture for innovative imaging and signal analysis in electrical tomography based on the construction of an electrical tomograph, measurement sensors and algorithms for data analysis [1-3]. Diseases of the respiratory and circulatory systems are common today. The development of this type of diseases (both acute and chronic) is influenced by many factors, including stress and environmental pollution. Early diagnosis, as well as the possibility of continuous monitoring outside the infirmary, is unfortunately not possible. The main objective of the project is to create a tomographic system for imaging and monitoring region of interest (ROI) using the node potential map, along with the mechanism of interpretation of disease states. The system will consist of a device that records the electrical potential of cardiac function and lung ventilation [4-5]. The system will monitor the patients' condition and support the diagnostic process in such diseases as:

- Chronic obstructive pulmonary disease (COPD)
- Acute respiratory failure syndrome (ARDS)
- Bronchospasm
- Obstructive sleep apnea (OSA)
- Pneumonia
- Pulmonary hypertension
- Pneumothorax
- Aortic insufficiency
- Cardiac Hemodynamics
- Ischemic heart disease
- Hypertension

24-hour monitoring of the vital functions of the patient is necessary for proper functioning. The future of medical diagnostics are long-term devices for patient monitoring - mobile devices that record a wide spectrum of diagnostics to detect pathological syndromes. The designed system will be able to monitor the following parameters:

- Myocardial activity
- Blood pressure
- Blood flow
- Impedance
- Heart rate
- Changes in pulmonary impedance
- Lung capacity
- ΔEELV (end-expiratory volume of lungs)
- Bio-impedance
- PEEP (positive end-expiratory pressure)
- Patient position during the test
- Relative electrical permittivity

Architecture

The concept of the system is based on the creation of a tomographic system for imaging and monitoring in the field using the map of node potentials and the mechanism of interpretation of disease states. The system consists of a data storage device and an aggregating and processing engine. The aggregation and processing engine will enable aggregation, processing and inference based on the collected data. For the purpose of medical inference for the reproduction of a tomographic image, algorithms are used to identify pathological syndromes and disease entities based on the collected data. All measurement signals are transmitted to the main module. The system will enable the acquisition of measurement data electrical impedance tomography (EIT) and electrical capacitive tomography (ECT), acquisition of electrocardiographic signals, impedance acquisition, pre-processing of measurement data, calibration of measuring elements (active electrodes), transmission of measurement data and power supply of active measuring electrodes [6-10]

The main module is an integral part of the mobile measuring device. Its functionality includes: acquisition of measurement data, initial processing of measured data, calibration of active electrodes, transfer of measurement data to the web-server system and power supply of the

entire system. The digital part of the main module is in progress. The analogue part will be created in the next two weeks. The block diagram of the measurement system is explained in Fig. 1. The patient is equipped with a measuring device with a sensor system. The signals are processed in the Analog Front-End analog module. Essentially, its task is to amplify the weak signal to the level required by the analog-to-digital converter (ADC) to ensure the desired quality of the digital signal. In addition, the module should provide pre-filtering of the signal. Then the digital signal is processed by the FPGA. Its basic functions include controlling the analog switch, switching the injection / measurement function, generating the signal for excitation and reading and processing signals in parallel.
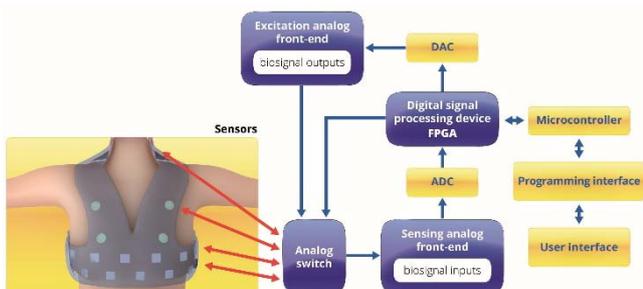

Fig. 1. Block diagram of the measurement system

The dominant solution when it comes to the electrode bearing system in EIT systems is the belt. The tape is fastened in a strictly defined position. At the moment, the measuring tape consists of two elastic belts connected together by means of the Velcro system, respectively a main belt with a width of 10 The electrodes are spread around the chest. For EIT measurements in medical applications, the electrode/skin interface is critical to achieving good results. In clinical trials, it most often uses electrodes made of silver or silver chloride. They provide excellent signal quality, but they have a serious disadvantage. To ensure good contact with the electrode and skin, use a special gel. However, it dries over time, causing a significant deterioration in the quality of the contact. Therefore, it should be replaced every few hours. In addition, the use of these electrodes usually requires patient preparation, i.e. the attachment sites must be shaved and disinfected with alcohol. The result is that these electrodes are not suitable for long-term use. In the case of our system, which is intended to monitor lung and heart function in long-term and outpatient settings, we must consider other options that will not require the use of gel while ensuring a signal quality comparable to that for Ag / AgCl. I'm talking about so-called dry electrodes. In general, dry electrodes can be divided into two groups: rigid and flexible electrodes. Rigid electrodes are usually made of metal, which provides good electrical properties, e.g. silver, aluminium, gold, titanium or stainless steel. They work well when the mounting site is attached and the patient does not move during the test. In our tomography, we must use flexible electrodes. Their main advantage is that they adapt much better to the shape of the body, and because of the greater adhesion, they reduce the impact of patient movements on the measured signal.

Image reconstruction

There are many methods to solve optimization problems [12-19]. In our work, we rely on deterministic algorithms [20-23]. Lung monitoring in unconscious intensive care patients, collecting data across the entire body boundary is impractical. The boundary area available for electrical

tomography measurements is limited. Physiological processes that cause changes in the electrical conductivity of the body can be monitored using hybrid algorithms. The proposed approach consists in solving a non-linear problem inverse to the reconstruction of the EIT image in which deterministic methods have been applied.

Regularization methods
Methods based on the SVD distribution

(1) $\quad \min_x \left\{ \|Ax - b\|_2^2 + \lambda^2 \|L(x - x^*)\|_2^2 \right\}$

In the case of EIT, we consider the sensitivity matrix as A, x the searched permittivity distribution, a b as a measurement vector. In regularization methods, the SVD or GSVD distribution can be used.
We are considering the distribution SVD ($A = U\Sigma V^T$) for $L = I$, and distribution GSVD

(2) $\quad A = U \begin{pmatrix} \Sigma & 0 \\ 0 & I \end{pmatrix} X^{-1}, L = V(M, 0) X^{-1}$ for $L \neq I$.

The case considered $L = I$.

Methods based on the SVD distribution
- Tikhonov method

For $x^* = 0$ we get a character solution

(3) $\quad x = \sum_{i=1}^{n} \frac{\sigma_i}{\sigma_i^2 + \lambda^2} u_i^T b v_i$

For $x^* \neq 0$

(4) $\quad x = \sum_{i=1}^{n} \frac{\sigma_i}{\sigma_i^2 + \lambda^2} u_i^T b v_i + \frac{\lambda_i^2}{\sigma_i^2 + \lambda^2} x^*$

- DSVD method

For $x^* = 0$ we get a solution

(5) $\quad x = \sum_{i=1}^{n} \frac{u_i^T b}{\sigma_i + \lambda_i} v_i$

For $x^* \neq 0$

(6) $\quad x = \sum_{i=1}^{n} \frac{u_i^T b}{\sigma_i + \lambda_i} v_i + \frac{\lambda_i}{\sigma_i + \lambda_i} x^*$

- TSVD method

We use matrix submatrices $U - U_\lambda = U(:,1:\lambda)$ and for the matrix $V - V_\lambda = V(:,1:\lambda)$.
For $x^* = 0$ we get a solution

(7) $\quad x = \sum_{i=1}^{\lambda} \frac{u_{\lambda i}^T b}{\sigma_i} v_{\lambda i}$
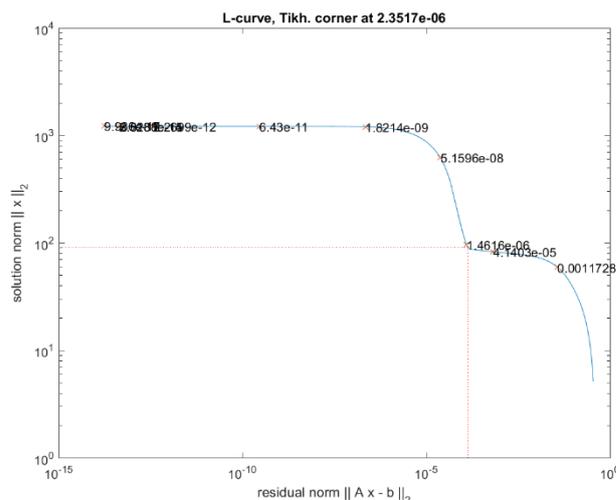

Fig. 2. Curve diagram L

For $x^* \neq 0$

(8) $\quad x = \sum_{i=1}^{\lambda} \left(\frac{u_{\lambda i}^T b}{\sigma_i} + v_{\lambda i}^T x^* \right) v_{\lambda i}$.

The parameter λ is supported by a curve L. The L curve determines the relationship between the solution's standard

and the residual norm for the specifically selected parameter range depending on the chosen method. Variables $u_i, v_i, u_{\lambda i}, v_{i\lambda}$ are the matrix columns respectively $U, V, U_\lambda, V_\lambda$. An example of the curve L curve is presented in Fig. 2.

Maximum entropy method

(9) $\quad \min_x \left\{ \left\| Ax - b \right\|_2^2 + \lambda^2 x^T \log(diag(w)\, x) \right\}$

It can obtain the equation

(10) $\quad 2A^T A + \lambda^2 \log x = 2A^T b - \lambda^2 \log w - \lambda^2$

We get a solution

(11) $\quad x = \frac{2A^T b - \lambda^2 \log w}{2A^T A + \lambda^2 I},$

for the approximation of the function $ax + \lambda^2 \log x \approx ax + \lambda^2 (x-1)$, in standardization. As before, the parameter was determined from the curve L. The weight vector was chosen as the average distance between the element and the electrodes.

Conjugate gradient method

(12) $\quad x_{k+1} = x_k + \alpha_k A^T b,$

where $\alpha_k = \frac{d_k^T d_k}{(A d_k)^T A d_k},$

(13) $\quad d_k = s + \beta_k d_{k-1}, \qquad d_0 = A^T b,$

(14) $\quad s_k = A^T r_k,$

(15) $\quad r_k = r_{k-1} - \alpha A d_k \qquad r_0 = b,$

(16) $\quad \beta_k = \frac{\rho_k}{d^T d},$

(17) $\quad \rho_k = s^T s, \qquad\qquad \rho_0 = d_0^T d_0.$

Reconstructions

For the presented methods, the values shown in Fig. 3. for the heart and lungs as a linear combination of the reciprocal of the absolute value from the logarithm of the values of the values have been adopted. These values have been transformed due to the method of regularization of maximum entropy.
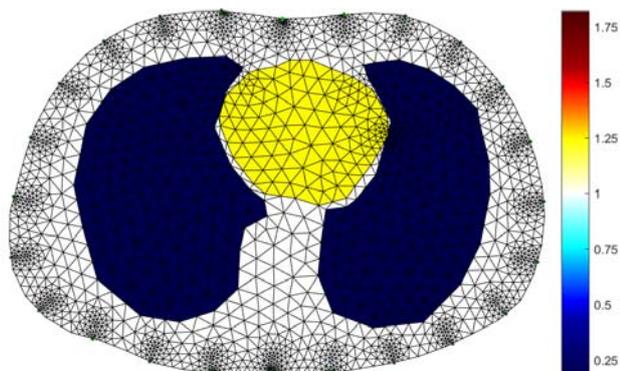

Fig. 3. 2D model of the lungs and heart

Figure 4 presents the image reconstruction by Tikhonov method. Algorithms based on the SVD distribution (Fig. 5-6) of the sensitivity matrix lead to similar reconstructions. However, the TSVD method (Fig. 5) leads to the worst reconstruction. This may be due to the fact that sub-masses determined by the parameter may not meet the Picard criteria. Figure 6 presents the image reconstruction by DSVD method.

Promising reconstructions were obtained by the methods of maximum entropy (Fig. 7) and the coupled gradient (Fig. 8). The lungs and the heart are clearly visible, but the difference between the permeability of these organs is also evident.
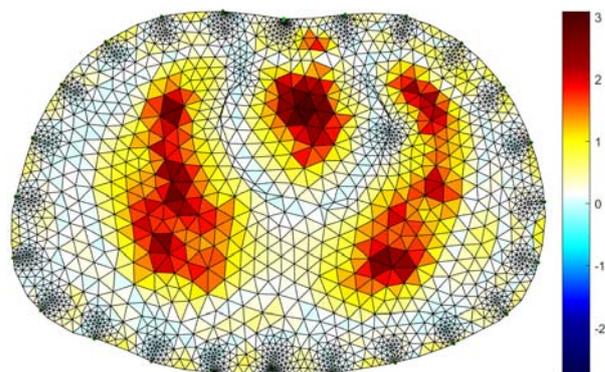

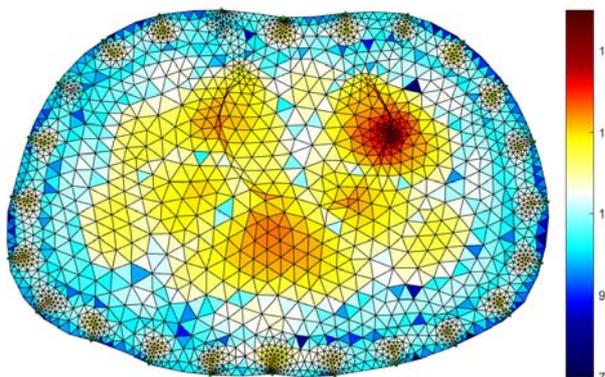Fig. 4. Image reconstruction by Tikhonov method

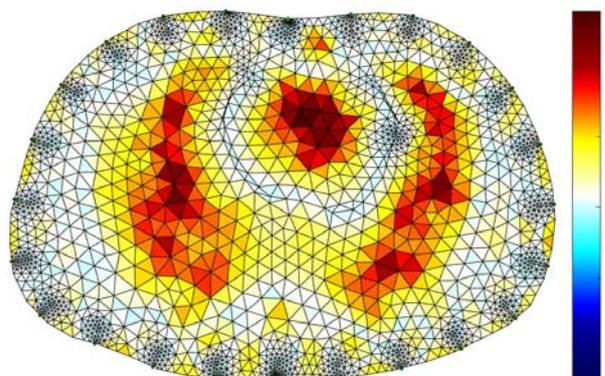Fig. 5. Image reconstruction by TSVD method

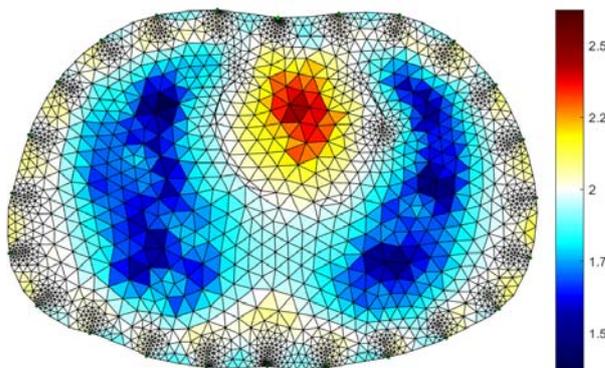Fig. 6. Image reconstruction by DSVD method

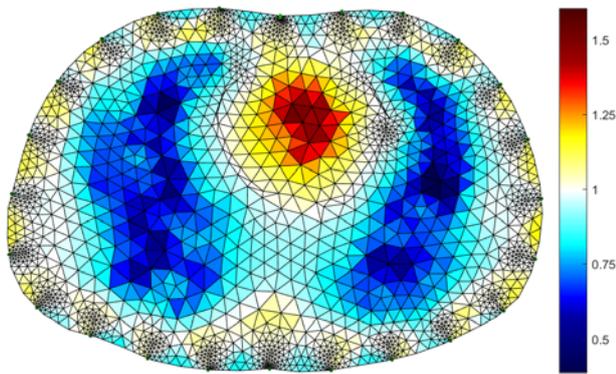Fig. 7. Image reconstruction by maximum entropy method

Fig. 8. Image reconstruction by conjugate gradient method

Summary

The article presents an advanced system of electrical tomography for the biomedical application. The architecture of the system based on electrical tomography has been implemented. In many applications of electrical tomography, such as lung monitoring of unconscious intensive care patients, acquiring data across the entire body boundary is impractical. The boundary area available for electrical tomography measurements is limited. Physiological processes that cause changes in the electrical conductivity of the body can be monitored using hybrid algorithms. The proposed approach was based on the solution of a non-linear inverse problem. To provide a high-level application programming interface using standard communication protocols and execute user-level programs. The platform consists of a data collection device and an aggregation and processing mechanism to generate useful information for diagnostic purposes or to pre-monitor physiological changes in the body. The deterministic algorithms based on the SVD distribution and gradient techniques for the lung and heart model were analysed. The applied algorithms of electrical reconstruction of impedance tomography solve the inverse problem with the appropriate accuracy.

Authors: Tomasz Rymarczyk, Netrix S.A., Phd. Eng, Research and Development Centre, Związkowa 26, 20-148 Lublin, University of Economics and Innovation in Lublin, ul. Projektowa 4, 20-209 Lublin, e-mail: tomasz@rymarczyk.com, Paweł Nita, Phd, Netrix S.A., Research and Development Centre, Związkowa 26, 20-148 Lublin, Andres Vejar, Phd, Netrix S.A., Research and Development Centre, Związkowa 26, 20-148 Lublin, Barbara Stefaniak, Netrix S.A., Research and Development Centre, Związkowa 26, 20-148 Lublin, ,Jan Sikora, Prof, Netrix S.A., Research and Development Centre, Związkowa 26, 20-148 Lublin,

REFERENCES

[1] Grudzien K., Romanowski A., Chaniecki Z., Niedostatkiewicz M., Sankowski D., Description of the silo flow and bulk solid pulsation detection using ECT, Flow Measurement and Instrumentation, 21 (2010), no. 3, 198-206
[2] Ye Z., Banasiak R., Soleimani M., Planar array 3D electrical capacitance tomography, Insight: Non-Destructive Testing and Condition Monitoring, 55 (2013), no. 12, 675-680
[3] Rymarczyk T., Kłosowski G., Application of neural reconstruction of tomographic images in the problem of reliability of flood protection facilities, Eksploatacja i Niezawodnosc – Maintenance and Reliability 20 (2018), no. 3, 425–434
[4] Searle A., Kirkup L., A direct comparison of wet, dry and insulating bioelectric recording electrodes, Physiological Measurement, 21 (2000), no. 2, 271
[5] Yapici M. K., Alkhidir T., Samad Y. A., Liao K., Graphene-clad textile electrodes for electrocardiogram monitoring, Sensors and Actuators B: Chemical, 221 (2015), 1469 – 1474
[6] Kryszyn J., Smolik W., Radzik B., Olszewski T., Szabatin R., Switchless charge-discharge circuit for electrical capacitance tomography, Measurement Science and Technology, 25 (2014), no. 11, 115009
[7] Mosorov V., Grudzień K., Sankowski D., Flow velocity measurement methods using electrical capacitance tomography, Informatyka, Automatyka, Pomiary w Gospodarce i Ochronie Środowiska (IAPGOŚ), 7 (2017), no. 1, 30-36
[8] Rymarczyk T., Kłosowski G., Kozłowski E., Non-Destructive System Based on Electrical Tomography and Machine Learning to Analyze Moisture of Buildings”, Sensors, 18 (2018), no. 7, 2285
[9] Wajman R., Fiderek P., Fidos H., Sankowski D., Banasiak R., Metrological evaluation of a 3D electrical capacitance tomography measurement system for two-phase flow fraction determination, Measurement Science and Technology, 24 (2013), no. 6, 065302
[10] Filipowicz S.F., Rymarczyk T. Measurement Methods and Image Reconstruction in Electrical Impedance Tomography, Przeglad Elektrotechniczny, 88 (2012), no. 6, 247-250
[11] Babout L., Grudzień K., Wiącek J., Niedostatkiewicz M., Karpiński B., Szkodo M., Selection of material for X-ray tomography analysis and DEM simulations: comparison between granular materials of biological and non-biological origins, Granular Matter, 20 (2018), no. 3, 20:38
[12] Fiala P., Drexler P., Nešpor D., Szabó Z., Mikulka J., Polívka J., The Evaluation of Noise Spectroscopy Tests, ENTROPY, 18 (2016), no. 12, 1-16
[13] Kłosowski G., Kozłowski E., Gola A., Integer linear programming in optimization of waste after cutting in the furniture manufacturing, Advances in Intelligent Systems and Computing 2018; 637 (2018), 260-270
[14] Kosicka E., Kozłowski E., Mazurkiewicz D., Intelligent Systems of Forecasting the Failure of Machinery Park and Supporting Fulfilment of Orders of Spare Parts, Advances in Intelligent Systems and Computing, 63 (2018), 54–63
[15] Polakowski K., Filipowicz S.F., Sikora J., Rymarczyk T., Tomography Technology Application for Workflows of Gases Monitoring in the Automotive Systems, Przeglad Elektrotechniczny, 84 (2008), no. 12, 227-229
[16] Ziolkowski M., Gratkowski S., Zywica A. R., Analytical and numerical models of the magnetoacoustic tomography with magnetic induction, COMPEL - The international journal for computation and mathematics in electrical and electronic engineering, 37 (2018), no. 2, 538–548
[17] Psuj G., Multi-Sensor Data Integration Using Deep Learning for Characterization of Defects in Steel Elements”, Sensors, 18 (2018), no. 1, 292
[18] Lopato P., Chady T., Sikora R., Ziolkowski S. M., Full wave numerical modelling of terahertz systems for nondestructive evaluation of dielectric structures, COMPEL - The international journal for computation and mathematics in electrical and electronic engineering, 32 (2013), no. 3, 736 – 749
[19] Mosorov V., Grudzień K., Sankowski D., Flow velocity measurement methods using electrical capacitance tomography, Informatyka, Automatyka, Pomiary w Gospodarce i Ochronie Środowiska (IAPGOŚ), 7 (2017), no. 1, 30-36
[20] Adler A., Lionheart W.R.B. Uses and abuses of EIDORS: an extensible software base for EIT, Physiological Measurement, 27 (2006), no. 5, 25–42
[21] Rymarczyk T., Sikora J., Applying industrial tomography to control and optimization flow systems, Open Physics, 16 (2018), 332–345
[22] Soleimani M., Mitchell CN,. Banasiak R., Wajman R., Adler A., Four-dimensional electrical capacitance tomography imaging using experimental data, Progress In Electromagnetics Research, 90 (2009), 171-186
[23] Dušek J., Hladký D., Mikulka J., Electrical Impedance Tomography Methods and Algorithms Processed with a GPU, In PIERS Proceedings, 2017, 1710-1714